THE ASTROPHYSICAL JOURNAL, Vol. 159, February 1970

THE SPECTRUM OF α^2 CVn. II

JUDITH G. COHEN*
Mount Wilson and Palomar Observatories, Carnegie Institution of Washington,
California Institute of Technology
Received 1969 June 5; revised 1969 July 14

ABSTRACT

The behavior of the continuum of α^2 CVn has been studied. The Balmer discontinuity does not vary but the slope of the Paschen continuum changes over the cycle. The line-blanketing coefficients have been measured at several phases and do not change sufficiently to produce the observed variations of the continuum. The effective temperature (12000° K) and surface gravity (log g = 4.0) are determined from the scans and hydrogen-line profiles, and the behavior of equivalent width as a function of phase is discussed. A crude abundance analysis is performed, which shows that the iron peak is enhanced above the solar value and that the rare earths are even more overabundant than was previously thought. The results of the abundance analysis are discussed in terms of a first-order oblique-rotator model, and the implications for the theory of Ap stars are described.

I. INTRODUCTION

The observational material on α^2 CVn described in Cohen, Deutsch, and Greenstein (1969, henceforth called Paper I) comprises a repository of useful data on this peculiar A star. In an effort to extract the maximum possible information, we have supplemented the spectra in the yellow and red by spectra in the blue, included continuum observations, and analyzed the whole body of observations within the framework of the oblique-rotator theory. We find this model to be consistent with all of the observations, but several puzzling aspects of the behavior of α^2 CVn remain to be explained. In § II the narrow-band photometry of the continuum is discussed, while § III deals with the equivalent widths as a function of phase. We determine the effective temperature and surface gravity in § IV. In § V the results of the abundance analysis are presented, and in § VI we discuss the consistency of these results with the oblique-rotator model. Section VII presents a brief summary of our conclusions.

II. THE NARROW-BAND PHOTOMETRY OF THE CONTINUUM

Spectrum scans with a 50 Å bandpass were made of α^2 CVn over a single period by Dr. J. B. Oke, who used the 100-inch Cassegrain scanner from May 14 through May 20, 1965. I am grateful to him for permission to analyze this material. The standard wavelengths suggested by Oke (1964) were used, with the calibration of Wolff, Kuhi, and Hayes (1968). At least three standard stars chosen from Oke's (1964) list were observed each night. The diaphragm was sufficiently small to avoid problems of contamination by α^1 CVn. For the blue region, 3400–5700 Å, seven scans are available at phases Φ = 0.03, 0.18, 0.58, 0.63, 0.67, 0.81, and 0.99. There are only two scans of the region 5000–11000 Å, at Φ 0.02 and 0.20.

Figures 1 and 2 show the average color indices with respect to 5550 Å of the blue scans, at the phases 0.25–0.75, and of the scans over the remainder of the period, as well as the average of the two red scans. The Balmer discontinuity does not appear to vary systematically, although the discrepancy between the scans is perhaps slightly larger than can be attributed to observational error. However, the slope of the Paschen continuum changes over the period, the star being reddest near rare-earth maximum at Φ = 0.0.

* National Science Foundation Trainee.

The *UBV* photometry of Pyper (1969) is consistent with the scanner observations. Although the absolute scale is less reliable, it appears that at 5550 Å the star is 0.1 mag brighter over that part of the period near $\Phi = 0.0$ than in the remaining half of the cycle.

Because it has been suggested that the role of differential line blanketing is crucial to the understanding of the photometric variation of α^2 CVn, we have measured the

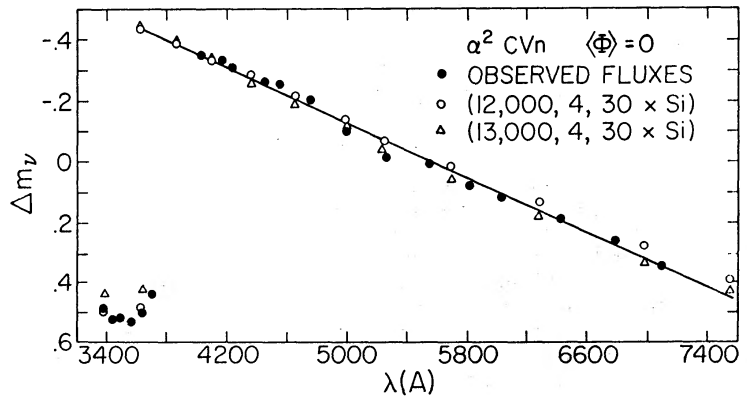

FIG. 1.—Observed fluxes per unit frequency for α^2 CVn at $\langle\Phi\rangle = 0.0$ compared with silicon-rich model atmospheres. *Solid line*, mean fit to observed points.

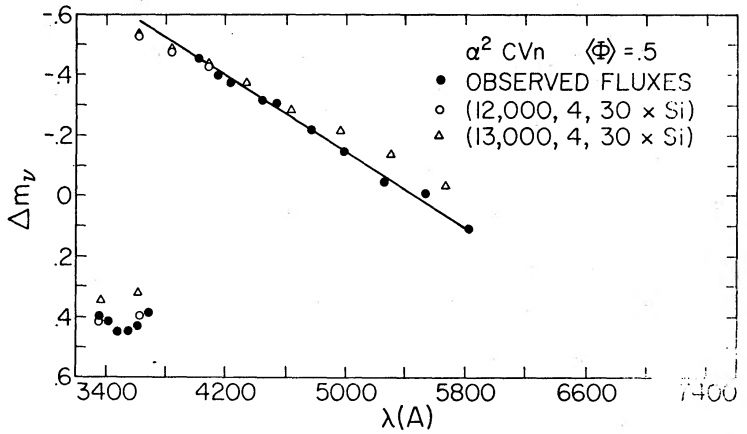

FIG. 2.—Observed fluxes per unit frequency for α^2 CVn at $\langle\Phi\rangle = 0.5$ compared with silicon-rich model atmospheres. *Solid line*, mean fit to the observed points.

blanketing coefficient η in the 50 Å bandpasses, around the cycle. If F_λ is the observed stellar flux and F_c is the flux in the continuum, then

$$\eta = \int_{\lambda_0-25\text{ Å}}^{\lambda_0+25\text{ Å}} F_\lambda d\lambda \Big/ \int_{\lambda_0-25\text{ Å}}^{\lambda_0+25\text{ Å}} F_c d\lambda \,. \qquad (1)$$

For this purpose, we used high-dispersion spectra taken by Dr. John Danziger and Dr. Peter Conti with the 100-inch coudé spectrograph for the blue region, and the spectra described in Paper I for the red.

Table 1 gives the values of η for α^2 CVn. For the red region, measurements were made on five plates evenly distributed over the period. The scatter at a fixed λ from phase to

phase was about 0.015, and we list average values of η. Since Melbourne (1960) finds the probable error due to random errors of measurement in η to be 0.01 mag, it would be impossible to detect any variation in η over the period. In the blue region, the dispersion of the spectra used was 4.5 Å mm^{-1}. Plates at three different phases were measured for each wavelength. In addition, several plates were measured at the same phase, namely, 0.02. Although the scatter is larger here, it is not more than 0.02, and any effect which might be due to a change in the line blanketing with phase is small compared with the scatter of the measurements from plate to plate at the same phase. Thus we again list average values of η in Table 1.

Several important conclusions follow from the above. First, the observed change in the continuum with phase is not due to a change in the distribution of the lines with phase, as any dependence of η on phase is smaller than the random errors in the measurements, i.e., less than 0.03 mag. Second, η is an anomalously flat function of wavelength. Although the results for $\lambda < 5000$ Å may not be directly comparable with those for $\lambda > 5000$ Å since the dispersion of the plates and hence the scale of the tracings were different in these two cases, a mere comparison of the blue measurement of η in α^2 CVn with those given by Melbourne (1960) shows the unusually strong blanketing encountered in the region 4000–5000 Å in the case of the Ap star. This same effect has to some

TABLE 1

LINE-BLANKETING COEFFICIENTS FOR α^2 CVn

(50 Å Bandpass)

λ(Å)	η(λ)	λ(Å)	η(λ)
3300.....	0.89	4460.....	0.92
3400.....	0.91	4566.....	0.92
3500.....	0.94	5000.....	0.95
3600.....	0.95	5264.....	0.94
3700.....	0.91	5546.....	0.95
4036.....	0.90	5840.....	0.96
4167.....	0.92	6056.....	0.96
4255.....	0.92	6426.....	0.97

extent been found by Wolff (1967). Note that the monochromatic magnitudes of Figures 1 and 2 have been corrected for line blocking by the mean values of η.

III. THE EQUIVALENT WIDTHS

Fourteen of the 6.7 Å mm^{-1} IIaD and IIaF plates described in Paper I were used for measuring equivalent widths, and a list of approximately 150 lines suitable for measurement was drawn up based on the identifications given and the relative scarcity of lines for a given ion. All unblended identified lines were measured.

Equivalent widths were obtained by planimetry of the tracings. The choice of continuum level was very difficult since the spectrum is so rich in lines. In order to maintain consistency from plate to plate, the same person chose the continuum level on all the tracings. The final probable errors in measurement for any given line can be estimated by comparing the equivalent widths at $\Phi = 0.64$, at which phase three plates were measured. They seem to be near 20 percent, except for lines with equivalent widths less than 40 mÅ, where the errors can be larger. The existence of such large photometric errors in the data is disappointing, but not surprising.

The next step in the reduction of the data is to determine the mean variation in line intensity with phase for each ion. Previous work by Deutsch (1958) has shown that in spectrum variables the ratio $W_\lambda/\bar{\omega}_\lambda$, where $\bar{\omega}_\lambda$ is the equivalent width averaged over the

period, is the same function of phase, to within the errors of observation, for all lines of a given element.

If we define $\langle \omega_\lambda \rangle$ as the average of W_λ (the observed equivalent width at a given phase) over all observed phases, we can correct $\langle \omega_\lambda \rangle$ in an approximate manner for the missing phases to obtain $\bar{\omega}_\lambda$. In Table 2 we list the $\bar{\omega}_\lambda$ for the lines whose equivalent widths were measured. For each line, the function $w = W_\lambda/\bar{\omega}_\lambda$ was tabulated as a function of phase. Because the errors of measurement are large, it is not surprising that a large range of values were obtained for lines of the same ion. For each ion we then averaged w over all lines of the ion where $\bar{\omega}_\lambda$ was greater than some previously chosen value (usually 15 or 30 mÅ) to obtain $\langle w \rangle$. Lines with smaller $\bar{\omega}_\lambda$ were rejected to avoid cases where either the errors of measurement of the equivalent widths were very large or the lines disappeared completely at certain phases. The final values of $\langle w \rangle$ as a function of Φ for each ion, as well as the number of lines used in forming the average, are listed in Table 3. The accuracy of the entries can be determined by comparing the results at phases 0.35 and 0.37, which should be almost identical. In this manner we see that the error in $\langle w \rangle$ due to the accumulated random errors in the equivalent widths is probably less than 15 percent. The systematic errors for all lines on all the plates have little effect on $\langle w \rangle$, which is a ratio of equivalent widths.

These are two cases where lines of more than one ion of a given element were measured. The form of $\langle w \rangle$ as a function of phase is the same for lines of Gd II and Gd III to within the observational error, which is large, since relatively few lines were observed for each ion. The same can be said for lines of Fe II and Fe I, where the curve for neutral iron is not well determined as only a few lines are present. Deutsch (1958) has shown that if the curve of growth can be approximated by a straight line, then w must be the same for all lines of the same element in the oblique-rotator model with a constant temperature and pressure over the surface. The equality of $\langle w \rangle$ for lines of two ions of the same element is thus to be expected if the oblique-rotator model is valid.

With such a large range in $\bar{\omega}_\lambda$ included in the lines we measured, it is somewhat surprising that the approximation of the curve of growth as a straight line is satisfactory. Indeed, there is some evidence that the approximation is not adequate. The function $\langle w \rangle$ for the strong Fe II lines $\bar{\omega}_\lambda > 100$ mÅ has a smaller amplitude than that for the weaker Fe II lines ($15 < \bar{\omega}_\lambda < 100$ mÅ). An even larger amplitude is obtained for Fe II lines with 15 mÅ $< \bar{\omega}_\lambda <$ 40 mÅ. It is possible that in the latter case the lines are near the linear part of the curve of growth over most of the surface, whereas the group of strong lines may, at some region of the visible hemisphere, be on the flat part of the curve, so that for the same ratio of iron number density at different phases, varying line ratios occur. The decrease in amplitude as $\bar{\omega}_\lambda$ increases can be predicted theoretically, by using the formalism for the oblique-rotator model developed by Deutsch (1958) with an approximation of the local equivalent width by polynomial $a\Sigma - b\Sigma^2$, where Σ is the local number density of atoms of the element producing the line.

The change in amplitude was noticed only for Fe II lines, and the differences between $\langle w(\Phi) \rangle$ for the strong and weak groups of lines are somewhat larger than the probable error in $\langle w(\Phi) \rangle$. Unfortunately, there is no other ion with a sufficient number of lines to allow us to try such an analysis. It is also possible that the change in amplitude is related to the separate components of Fe II lines found by Pyper (1969). Note that if the curve of growth for the four components can be represented by a single straight line, then $w(\Phi)$ should be identical for all lines. But the line doubling was not resolved on our spectra, and there may be a systematic error in the determination of the profiles of the weak doublets as compared with the stronger ones.

IV. THE EFFECTIVE TEMPERATURE AND SURFACE GRAVITY

We now attempt to determine the effective temperature and surface gravity of α^2 CVn. Previous studies have indicated that the presence of the magnetic field does not affect

TABLE 2

W_λ FOR α^2 CVn

Line	$\bar{\omega}_\lambda$ (mÅ)	Line	$\bar{\omega}_\lambda$ (mÅ)	Line	$\bar{\omega}_\lambda$ (mÅ)	Line	$\bar{\omega}_\lambda$ (mÅ)
C II		Ti I		Fe II		Sm II	
6578.0	< 10	5512.5	14	5813.7	63	6182.9	10
N II		5644.1	48	5952.6	46	6267.3	10
5679.6	< 10	5675.4	24	6084.1	31	Eu II	
O I		Ti II		6113.3	33	5966.1	30
6156.8	10	5129.1	20	6147.7	75	6049.5	49
6158.2	87	5336.8	31	6247.6	108	6173.1	10
Ne I		V II		6332.0	60	6437.6	10
6402.2	< 10	5106.2	66:	6416.9	87	6645.1	10
Na I		5241.2	84:	6433.9	44	Gd II	
5889.9	< 10	Cr II		6456.4	110	5108.9	10
5895.9	< 10	5237.3	62	Y II		5733.9	12
Si II		5275.0	70	5205.7	50	5749.4	10
5041.0	247	5308.4	63	5546.0	26	5820.9	10
5056.0	361	5478.4	81	5662.9	10	5877.3	10
5800.5	45	5508.6	43	La II		6380.9	11
5868.4	73	Mn I		5080.2	10	Gd III	
5957.6	138	5337.6	16	5566.9	10	5091.7	20
5978.9	155	5551.9	10	5671.6	24	5553.3	15
6347.1	360	Mn II		5874.0	10	5608.9	30
6371.4	295	5294.2	78	Ce II		5665.2	25
6671.9	59	Fe I		5235.8	37	5724.7	10
P II		5027.1	57	5417.8	14	5862.1	10
6043.1	< 10	5048.5	46	5472.3	40	6014.8	20
6034.0	< 10	5125.1	18	5518.5	12	6065.7	12
6024.2	< 10	5383.4	56	Pr II		6198.9	27
S II		5554.9	43	5206.6	10	Hg I	
5428.6	19:	5557.9	31	5220.1	33	5460.7	< 10
5556.0	< 10	5586.8	87	5292.1	27	Pb II	
5606.1	41:	Fe II		5322.8	10	5042.5	< 10
5645.6	65:	5018.4	209	5687.2	10		
Cℓ II		5036.9	150	Pr III			
5078.3	18	5169.0	177	5300.0	79		
5217.9	35	5180.5	47	5765.3	14		
5221.4	62	5197.6	100	Nd II			
5392.1	10	5234.6	146	5548.5	38		
5423.4	22	5272.4	62	5804.0	27		
5443.4	40	5276.0	102	6183.9	12		
5444.2	59	5284.1	157	Sm II			
5457.1	18	5325.6	88	5537.1	31		
A I		5362.9	125	5831.7	12		
5495.9	< 10	5414.1	61	5938.9	10		
		5525.1	44	6168.3	18		
		5534.9	132	6181.1	10		

the continuum, so that we may use model atmospheres for nonrotating stars with zero magnetic field.

We shall use the grid of models computed under the assumption of radiative equilibrium and LTE by Strom and Strom (1969) in a study of the ultraviolet opacity of Si I. We designate models by ($T_{\rm eff}$, log g, abundance of Si in terms of model/solar Si abundance). The maximum overabundance of Si considered by the Stroms was a factor of 30, which is less than the abundance of Si in α^2 CVn.

The most sensitive indication of effective temperature around B8 is the Balmer discontinuity. The photoelectric scans show that the Balmer discontinuity does not vary greatly with phase. From Figures 1 and 2 we determine $T_{\rm eff}$ of 12000° ± 500° K for the 30 × Si models. The uncertainty is based on the uncertainties in the observation and also in the absolute calibration near the Balmer discontinuity. The effective temperature can also be obtained from the slope of the Paschen continuum. However, the uncertainty by several hundredths of a magnitude in the absolute calibration of this region introduces a large uncertainty into the temperatures. Furthermore, the slope of the Paschen continuum varies with phase in a manner not as yet understood; it seems clear, from the behavior of the hydrogen lines and the phase relationships for the continuum

TABLE 3

$\langle w \rangle$ FOR α^2 CVn

Ions	Phase									No. of Lines
	0.04	0.22	0.35	0.37	0.49	0.53	0.59	0.64	0.84	
Gd II, Sm II, Pr II, Yb II	1.18	0.90	0.80	0.76	0.77	0.52	0.59	0.97	1.07	13
Gd III	1.33	0.93	0.50	0.61	0.63	0.85	1.00	0.88	1.31	5
Gd II	1.59	0.66	0.51	0.70	0.85	0.35	0.39	1.00	1.12	3
Si II	0.82	1.13	1.22	1.06	1.15	0.96	1.39	1.09	0.71	10
Fe II ($\bar{\omega}_\lambda > 100$)	0.89	1.04	1.09	0.98	1.15	1.01	1.11	1.10	0.95	10
Fe II ($15 < \bar{\omega}_\lambda < 100$)	0.77	1.18	1.28	1.07	1.18	0.99	1.13	1.14	0.76	19
Fe I	0.67	1.09	1.15	1.04	1.27	0.86	1.42	1.12	0.99	5
Cr II	0.74	1.25	1.25	1.07	1.14	1.00	0.99	1.11	0.79	8

at various wavelengths, that the variation of the Paschen continuum is not caused by a variation in the effective temperature of the star (see Paper I and Pyper 1969). We thus regard the slope of the Paschen continuum as an unreliable indication of $T_{\rm eff}$. We note that the $T_{\rm eff}$ implied by the Paschen continuum ranges from 12500° K at $\Phi = 0$ to 13500° K at $\Phi = 0.5$ for the 30 × Si models, so that at least these numbers are quite close to the effective temperature deduced from the Balmer discontinuity.

The surface gravity can be obtained from the profiles of the hydrogen lines. A profile of Hγ was given by Burbidge and Burbidge (1955), and S. E. Strom has kindly made available a photoelectric Hβ profile taken with the solar telescope at Kitt Peak. These profiles are compared with models in Figures 3 and 4. The principal uncertainty here is the broadening theory for the hydrogen lines; profiles for the Griem (1967) and Edmonds, Schlüter, and Wells (1967) theory are given. We see that the model (12000°, 4, 30 × Si) fits both lines satisfactorily and that the surface gravity log g is 4.0 ± 0.3. We note that the uncertainty in the profiles introduced by the broadening theory is small compared with the changes in the profiles produced by a change of 0.5 in log g. The equivalent width of Hγ given by Burbidge and Burbidge (1955) also agrees with that predicted by the (12000°, 4, 30 × Si) model. The Hγ profile varies slightly with phase, but not enough to change significantly the deduced surface gravity. Since only one Hβ scan was available, we do not know if this also varies.

The principal uncertainty in the models concerns the ultraviolet opacity. Strom and Strom have shown that the ultraviolet opacity of Si I can be important in this temperature range if that metal is greatly overabundant. In the peculiar A stars, many other elements are enhanced, and it is possible that they also contribute to the opacity in the ultraviolet. Strom and Strom, however, indicate that the temperature-pressure relationship for the models (11000°, 4, 30 × Si) is identical with that of the model (12000°, 4,

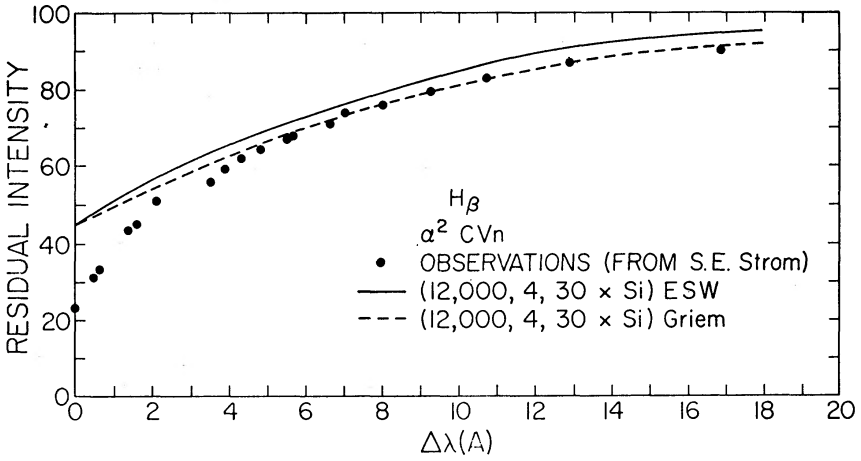

FIG. 3.—Observed Hβ profile compared with profiles computed for the same model atmosphere by using different theories of line broadening.

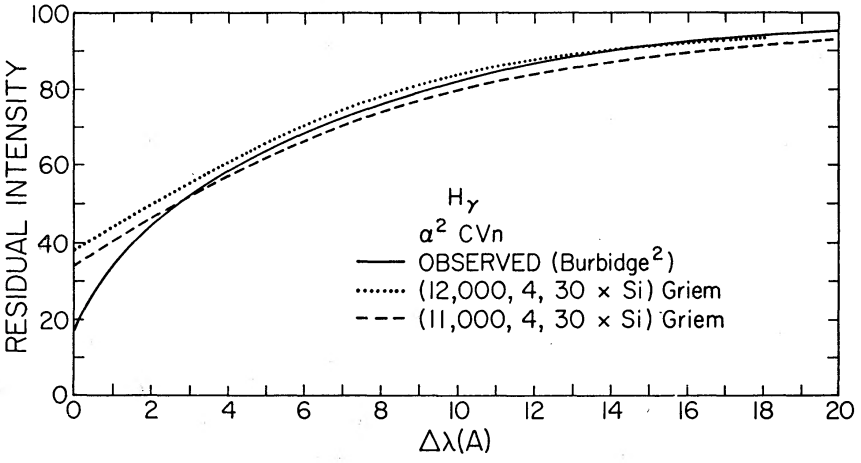

FIG. 4.—Observed Hγ profile compared with profiles computed for two model atmospheres

1 × Si), and these two models have the same continuum colors. Thus these two models will predict the same line strengths for the hydrogen lines as well as for all lines except those of silicon. Hence, to a first approximation, though we may overestimate the effective temperature of the star by using a model with only 30 times the solar Si content, we will obtain the correct abundances. In the extreme outermost layers of the atmosphere, there is some divergence between the two models discussed above, in that the boundary temperature is lower for the model with more silicon. This effect may perhaps be of some importance.

We therefore find that the atmosphere of α^2 CVn is best represented by the model

(12000°, 4, 30 × Si) which is approximately equivalent to the model (13000°, 4.0, 1 × Si). This choice of parameters describing the atmosphere is within the range of previous determinations by Searle and Sargent (1964), Jugaku and Sargent (1968), and Mihalas and Henshaw (1966).

V. THE ABUNDANCE ANALYSIS

The only previous abundance analysis of α^2 CVn was that of the Burbidges (1955, henceforth denoted by B^2). As Sargent (1964) points out, a reanalysis would be very useful as many new laboratory data are available, especially for the rare earths. Furthermore, the Burbidges used an effective temperature of about 10000° K, whereas modern values, with the exception of Wolff (1967), are about 2000° K hotter. The additional material in the yellow and red regions of the spectrum, together with the new identifications of Paper I, reduces somewhat the problem of blending.

We have made a first reconnaisance of the problem by neglecting any effects of the magnetic field or of horizontal separation of the elements (patches). We tried to make a crude abundance analysis in the quickest possible manner, using equivalent widths averaged over the phases 0.25–0.75 and over the remainder of the cycle, to get an average estimate of abundances in the hemisphere visible at mean phases 0.0 and 0.5. Because of the availablity of a program by S. E. Strom and R. L. Kurucz to compute equivalent widths from model atmospheres, the quickest method for a crude abundance analysis was that of a model-atmosphere analysis as described in Strom, Gingerich, and Strom (1966).

The gf-values have been compiled from many sources, and are in most cases not very accurate. We had to omit many lines from the analysis as no transition probabilities were available. If we could not find a gf-value for even one of the observed lines of an ion, we set $\log gf = -1.0$. Because of the great uncertainty in the absolute scale of transition probabilities, we have compared the results obtained for α^2 CVn with abundances deduced from the same set of lines and gf-values in a standard star. Unfortunately, no one star is suitable as a standard, as no normal star with such a high effective temperature has rare-earth lines of measurable strengths. Therefore, several stars were used, each of which has been shown to be normal when compared with the Sun. The primary standard was Vega, and the W_λ given in Strom, Gingerich, and Strom (1966) were used. For the rare earths, we were forced to use the Sun as a standard. The standard star for lines of high excitation not seen in Vega, such as Cl II or Ne I, was γ Peg, and the equivalent widths of Aller and Jugaku (1958) were used. In all cases, four stages of ionization were considered. The second ionization potentials of the rare earths are all known (Sugar and Reader 1965), and we have adopted 22 eV (as suggested by Sugar 1966) as the third ionization potential for a rare earth, if it has not yet been measured. The partition function for the higher ions of the rare earths was taken as the statistical weight of the ground state, since the laboratory data are inadequate for a more detailed treatment. The microturbulent velocity was set equal to zero.

The results of such a procedure are given in Table 4. There we give the logarithm of the ratio of the abundance relative to H in α^2 CVn to the abundance relative to H in the standard star. If no variation in the equivalent widths was detectable, we list the abundance in the first column. If, however, a variation was seen, we give the two abundances obtained from W_λ averaged over each half of the cycle. Since the temperature of the star is somewhat uncertain, we also list the change in the abundance that would result from a reduction in $T_{\rm eff}$ of α^2 CVn by 1000° K. If no lines have been observed in α^2 CVn for ions of interest, then upper limits are given to the abundance. Values which are unusually uncertain, primarily because of doubtful identifications, are indicated by a colon. For the ions Hg I, Hg II, Pb II, and Pr III where no lines could be found in any of the standard stars, we give the logarithm of the abundance of the element relative to hydrogen as determined with the adopted gf-values (gf for Hg I λ5460 is given in Corliss

and Bozman 1962, while the values used for lines of the other ions listed were adopted as $\log gf = -1.0$). The Pr III abundance is given relative to the solar abundance of Pr as determined from lines of Pr II in the solar spectrum.

We note that in some cases there were inadequate numbers of lines of an ion past 5000 Å, and we have supplemented our data with equivalent widths from B². The usual systematic effect of the lower-dispersion plates used by B² producing larger equivalent widths seems to be present, in that abundances deduced from lines in the blue taken from B² tend to be higher by up to 0.4 in the logarithm than were those obtained from lines in the red. A correction to any abundances obtained from data of B² has therefore been applied.

TABLE 4

FINAL ABUNDANCES FOR α^2 CVn

Ion	$\log (N/N_H)_* - \log (N/N_H)_{Standard}$ $\langle\Phi\rangle=0$	$\langle\Phi\rangle=0.5$	Δ for $\Delta T_{eff}=-1000°$ K	Ion	$\log (N/N_H)_* - \log (N/N_H)_{Standard}$ $\langle\Phi\rangle=0$	$\langle\Phi\rangle=0.5$	Δ for $\Delta T_{eff}=-1000°$ K
He I.....	<−1.7	...	...	Mn I....	+3.0	...	−0.2
C II.....	< 0.0	...	...	Mn II....	> 0	...	...
N II.....	<+1.3	...	...	Fe I.....	+1.6	1.9	−0.3
O I.....	+0.1:	...	−0.1	Fe II.....	+1.7	2.1	−0.1
Ne I.....	<+0.1	...	...	Sr II.....	+2.0:	...	−0.4
Na I.....	<−0.6	...	...	Y II.....	+2.9	2.7	−0.3
Mg II.....	−0.2:	...	0.0	Zr II.....	+2.2	1.8	−0.3
Al I.....	+1.1:	...	−0.4	Ba II....	<+1.6	...	...
Si II.....	+1.6	+1.9	+0.1	La II.....	+2.5	2.2	−0.3
P II.....	<+0.2	...	...	Ce II....	+4.2	3.7	−0.3
S II.....	< 1.8	...	...	Pr II.....	+4.3	3.5	−0.4
Cl II.....	+2.6	+1.6	+0.2	Pr III....	+3.0:	...	−0.1
Ar I.....	< 1.2	...	...	Nd II....	+4.2	...	−0.4
Ca I.....	+1.8:	...	−0.8	Sm II....	+3.9	3.4	−0.4
Ca II.....	−1:	...	−0.3	Eu II....	+6.2	5.0	−0.6
Sc II.....	1.9:	...	−0.5	Gd II....	+4.8	4.1	−0.5
Ti I.....	+2.6	...	−0.5	Dy II....	+4.3:	3.8:	−0.4
Ti II.....	+1.6	+1.3	−0.3	Hg I.....	<−7.5 abs.	...	...
V II.....	+2.5:	...	−0.3	Hg II....	<−9 abs.	...	...
Cr I.....	+1.9	+2.2	−0.5	Pb II....	<−6.5 abs.	...	...
Cr II.....	+1.7	+2.4	−0.2				

The ionization equilibrium as determined from two ions of Fe and Cr is quite satisfactory. Ti, Mn, Pr, and Ca are much less reliable, and it is not surprising that the agreement is much worse. If a large scatter from line to line is allowed for, there is no obvious systematic dependence of the deduced abundance on equivalent width on an excitation potential. This implies that our choices of temperature and microturbulent velocity are not grossly incorrect.

The abundance of O I is uncertain, as one of the two observed lines is blended. An approximate removal of the blend yields results in good agreement with those obtained by Sargent and Searle (1962) from the infrared triplet. Our Mg abundance also agrees with that determined by Sargent and Searle (1962). The question of Ca is very vexing. The line at λ4226, which was the only feature attributed to Ca I by the Burbidges, may well be Sm III. The only means of determining the Ca abundance is then the H- and K-lines, which are sensitive to temperature. It is still not clear whether the abnormal weakness of the H- and K-lines usually noted when classifying Ap stars is due either to the low temperature (too late a spectral class) or to a real anomaly in the calcium abundance. We note that the Pr II and Pr III lines do not give wildly inconsistent results when one recalls that the gf-value for lines of Pr III, as well as the third ionization potential of this element, were chosen arbitrarily since no laboratory data were available.

Bengston (1968) has measured transition probabilities for lines of Cl II. When we use these *gf*-values, our absolute abundance for chlorine (log N_{el}/N_H) in γ Peg is -6.5, which is somewhat lower than Aller's (1961) corrected value of -5.8 and tends toward the meteoritic abundance of about -7.1.

Several points of special interest stand out in the final abundance results. The region around chlorine shows P, S, Ar, and Ca not extremely anomalous, while Cl is vastly enhanced. It is difficult to imagine a nuclear process which will have such a narrow range of efficient operation in the periodic table. Furthermore, no element lighter than Cl is unusually overabundant, while nearly all elements heavier than Ca are overabundant. The whole iron peak is enhanced, in contrast with the results of B². In addition, the rare earths are more overabundant than determined by B², by factors of about 100. These differences between our results and those of B² are largely due to the higher effective temperature we have adopted.

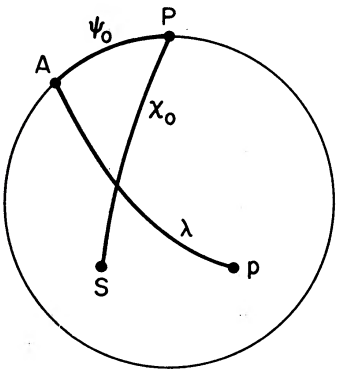

FIG. 5

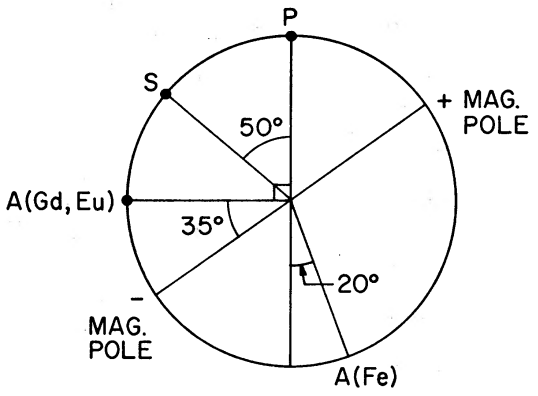

FIG. 6

FIG. 5.—Geometry of the oblique rotator. *P*, rotation axis; *S*, subsolar point; *A*, abundance pole.

FIG. 6.—Results of the first-order harmonic analysis. A cross-section in the meridional plane at $\Phi = 0.0$ and the positions of the abundance poles for the rare earths and Fe are shown.

VI. CONSISTENCY WITH THE OBLIQUE-ROTATOR MODEL

Pyper (1969) has given a complete harmonic analysis of her data using the oblique-rotator model and the formalism developed by Deutsch (1958). Because of the scatter in our data and the poor distribution of our plates over the period, we feel that a first-order harmonic analysis is sufficient. We therefore follow an analysis of Deutsch (1969), representing

$$w = \frac{W_\lambda}{\bar{\omega}_\lambda} = 1 + D \cos \Phi \tag{2}$$

and

$$\zeta = A + A \cos \lambda , \tag{3}$$

where ζ is the local equivalent width, and the element is assumed to be distributed over the surface with a maximum concentration at one point A and zero abundance at the opposite pole.

In Figure 5, P is the pole of the rotational axis, p is a point on the surface, and S is the subsolar point. D is then a known function of ψ_0 and χ_0. We may determine D from the data given in Table 3. Since χ_0 is known from previous work (we adopt Pyper's [1969] value of 50°), we can determine the angle ψ_0 and hence the location of the abundance pole for each element whose variations in equivalent width have been measured. Deutsch (1969) has shown that the largest possible value for D is 0.72, and, indeed, none

of the determined values exceed this limit. However, the maximum value of D depends on the angle of inclination, and for $\chi_0 = 50°$, D_{max} is somewhat less than the value indicated by the observations of the rare earths, $D = 0.55$. This is probably an indication of the importance of the second-order terms.

We have applied this treatment to the two best-observed elements. The rare earths are treated as a group, as are also the weak Fe II lines, which have a $w(\Phi)$ almost identical with that of the Fe I and Cr II lines and hence will give the same local concentrations. The results are shown in Figure 6, which is a cross-section in the meridional plane at $\Phi = 0.0$. The inclination of the magnetic axis, indicated for completeness but not used in the analysis, was taken from Pyper's (1969) analysis.

Even in this vastly simplified case the main features of Pyper's (1969) result emerge. The rare earths are concentrated in a region near the negative magnetic pole, and the iron-chromium group, in a region on the magnetic equator. Because we have not been able to resolve the components of the lines of group B studied by Pyper (1969), we felt that to construct a model without axial symmetry of the element concentration would be overanalyzing the available data.

We can integrate equation (2) over the visible hemisphere and over the period to obtain $\bar{\omega}_\lambda$ as a function of A and the orientation angles χ_0 and ψ_0. These angles are known from the above discussions, and hence we can obtain $2A$, which is the local equivalent width at the abundance pole. From this we can determine the local abundance at this pole, which is 8 times the abundance from $\bar{\omega}_\lambda$ for Fe and Cr, and 23 times the abundance from $\bar{\omega}_\lambda$ for Eu and Gd. Thus, in the simple model, the ratio of maximum to minimum abundance over the surface is infinite, and the maximum abundance is 23 and 8 times the mean abundance for elements of groups A and B, respectively. Element separation over the surface of roughly this magnitude must be obtained by any model which seeks to reproduce the anomalous behavior of α^2 CVn.

We have confirmed the result of Pyper (1969) that the rare earths are strongly concentrated near the negative magnetic pole, yet no strong concentration is found near the positive magnetic pole. It is difficult to imagine a separation mechanism which depends not only on the strength of the magnetic field but also on its sign.

We are not convinced that nuclear processes are responsible for the observed abundances. There is the problem of the sharp peak in abundance at chlorine, with no such extreme enhancement of the neighboring elements. The fact that the enhancement of the rare earths is much greater than any possible enhancement of Ba or Pb is difficult to overcome in a nuclear theory. If we add up all the excesses, in terms of the fraction of the star which has been transformed into elements heavier than helium, then we find that the dominant contributions are from chlorine and silicon; roughly 0.1 percent of the atoms in the photosphere are of these two elements. However, helium, which may be completely absent from the photosphere, is normally 10 percent of the atoms in the photosphere. Therefore, if nine helium atoms were put together to form Cl or Si, and if all of the helium were processed, then there would be an abundance of these elements 10 times greater than that observed.

With regard to processes of vertical stratification, such as that recently suggested by Michaud (1969), we can calculate the depth to which a process might occur by adopting a simple exponential pressure law with a constant scale height and using the maximum observed overabundance (that of Eu). If we require all the Eu (assumed to be of normal solar abundance) down to a depth of 13 scale heights to be concentrated in a layer 1 scale height thick at the photosphere, we produce the observed mean abundance of Eu, $10^{5.5}$ times the solar value. Thus, if the radius of α^2 CVn is 4 $R_\odot$, then material from the surface to a depth of $\frac{1}{350} R$ must be subjected to complete vertical stratification. If the patches are very small and thin, the depth to which the stratification must operate is greatly reduced; however, this seems inconsistent with the spectroscopic data. From our results it is clear that the stratification mechanism is not dependent only on mass or on the ratio of charge to mass of the dominant ion of an element.

VII. CONCLUSIONS

The oblique-rotator model for peculiar A stars is consistent in all respects with the observations of α^2 CVn. There remain, however, two problems which seem to defy solution. The first is the problem of the color variations of the continuum, which cannot be explained by line blanketing. Furthermore, while it is clear that there must be patches of different concentrations over the surface which itself is at an approximately uniform temperature and pressure, the mechanism giving rise to the differing horizontal separation of the elements is still unclear.

I thank the late Dr. Armin J. Deutsch for constant advice and encouragement. I thank Drs. Peter Conti, A. J. Deutsch, I. J. Danziger, J. L. Greenstein, J. B. Oke, and S. E. Strom for contributing observational material. Special thanks are due to Robert Kurucz and Dr. S. E. Strom for the use of their computer programs. I am indebted to Jon Okada for his help in the measurements, and to Mrs. Naomi Greenstein for improving the manuscript.

REFERENCES

Aller, L. H. 1961, *The Abundance of the Elements* (New York: Interscience Publishers), p. 194.
Aller, L. H., and Jugaku, J. 1958, *Ap. J.*, **127**, 125.
Bengston, R. D. 1968, University of Maryland Technical Note BN-559.
Burbidge, G. R., and Burbidge, E. M. 1955, *Ap. J. Suppl.*, **1**, 431.
Cohen, J. G., Deutsch, A. J., and Greenstein, J. L. 1969, *Ap. J.*, **156**, 629.
Corliss, C. H., and Bozman, W. R. 1962, *N.B.S. Monog.*, No. 53.
Deutsch, A. J. 1958, *Proc. I.A.U. Symp. No. 6*, p. 209.
———. 1969 (private communication).
Edmonds, F. N., Jr., Schlüter, H., and Wells, D. C., III. 1967, *Memoirs R.A.S.*, **71**, 271.
Griem, H. R. 1967, *Ap. J.*, **147**, 1092.
Jugaku, J., and Sargent, W. L. W. 1968, *Ap. J.*, **151**, 259.
Melbourne, W. G. 1960, *Ap. J.*, **132**, 101.
Michaud, G. 1969 (to be published).
Mihalas, D., and Henshaw, J. L. 1966, *Ap. J.*, **144**, 25.
Oke, J. B. 1964, *Ap. J.*, **140**, 689.
Pyper, D. 1969, *Ap. J. Suppl.*, **18**, 347.
Sargent, W. L. W. 1964, *Ann. Rev. Astr. and Ap.*, **2**, 297.
Sargent, W. L. W., and Searle, L. 1962, *Ap. J.*, **136**, 408.
Searle, L., and Sargent, W. L. W. 1964, *Ap. J.*, **139**, 793.
Strom, S. E., Gingerich, O. J., and Strom, K. M. 1966, *Ap. J.*, **146**, 880.
Strom, S. E., and Strom, K. M. 1969, *Ap. J.*, **155**, 17.
Sugar, J. 1966, quoted by Bidelman in *The Magnetic and Related Stars*, ed. R. C. Cameron (Baltimore: Mono Book Co.), p. 38.
Sugar, J., and Reader, J. 1965, *J. Opt. Soc. Am.*, **55**, 1286.
Wolff, S. C. 1967, *Ap. J. Suppl.*, **15**, 21.
Wolff, S. C., Kuhi, L. V., and Hayes, D. 1968, *Ap. J.*, **152**, 871.